



# Geophysical methods help to assess potential groundwater extraction sites

Helga Wiederhold<sup>1</sup> · Anders Juhl Kallesøe<sup>2</sup> · Reinhard Kirsch<sup>3</sup> · Rebekka Mecking<sup>4</sup> · Renate Pechnig<sup>5</sup> · Frank Skowronek<sup>6</sup>

Received: 27 January 2021 / Revised: 14 May 2021 / Accepted: 19 May 2021 / Published online: 7 October 2021  
© The Author(s) 2021

## Abstract

Complex geology in glacial terrain makes groundwater exploration challenging for water supply companies. Abrupt lateral changes of geological conditions, for example, raise the risk of unsuccessful exploration drilling. At some locations, local water supply companies experience a large number of dry wells, raising the need for better exploration approaches. The use of geophysical techniques enables the detection and characterization of subsurface structures in terms of aquifers and aquitards.

We present two examples in which seismic and resistivity methods are combined for subsurface characterization. A thrust structure is detected in the Varde study area in Denmark and a channel structure is mapped in the Hamburg-Sülldorf study area in Germany. The different imaging characteristics of seismic P- and S-waves are demonstrated. The combination of seismic and resistivity methods enables delineating groundwater-bearing and groundwater-barrier layers down to a depth of 150 m.

**Keywords** Seismic reflection · Electrical resistivity · P-waves · S-waves · Geophysics

## Geophysikalische Methoden zur Bewertung potenzieller Standorte für die Grundwassergewinnung

### Zusammenfassung

Eine komplexe Geologie in glazial geprägtem Untergrund fordert Wasserversorger bei der Grundwassererkundung heraus. Extrem veränderliche geologische Bedingungen erhöhen das Risiko erfolgloser Aufschlussbohrungen. An einigen Standorten erleben lokale Wasserversorger eine große Anzahl von Fehlbohrungen und fragen nach weiteren Aufsuchungsmethoden. Die Anwendung geophysikalischer Methoden ermöglicht die Entdeckung und Charakterisierung von Untergrundstrukturen bezüglich Grundwasserleiter und undurchlässiger Schichten.

---

✉ Helga Wiederhold  
helga.wiederhold@leibniz-liag.de

Anders Juhl Kallesøe  
ajk@geus.dk

Reinhard Kirsch  
geo-i@mytng.de

Rebekka Mecking  
rebekka.mecking@leibniz-liag.de

Renate Pechnig  
r.pechnig@geophysica.de

Frank Skowronek  
frank.skowronek@hamburgwasser.de

<sup>1</sup> Leibniz Institute for Applied Geophysics (LIAG), Stilleweg 2, 30655 Hannover, Germany

<sup>2</sup> Geological Survey of Denmark and Greenland (GEUS), C.F. Müllers Allé 8, 8000 Aarhus C, Denmark

<sup>3</sup> Geoimpulse, Graf-Spee-Str. 4–6, 24105 Kiel, Germany

<sup>4</sup> Leibniz Institute for Applied Geophysics (LIAG), Stilleweg 2, 30655 Hannover, Germany

<sup>5</sup> Geophysica Beratungsgesellschaft mbH, Lütticher Straße 32, 52064 Aachen, Germany

<sup>6</sup> Hamburger Wasserwerke GmbH, Billhorner Deich 2, 20539 Hamburg, Germany

Wir stellen zwei Beispiele vor, bei denen Seismik und elektrische Verfahren für eine Untergrundcharakterisierung kombiniert werden. Im Projektgebiet Varde in Dänemark wird eine Überschiebungsstruktur aufgedeckt und im Projektgebiet Hamburg-Sülldorf (Deutschland) wird eine Rinnenstruktur abgebildet. Das unterschiedliche Abbildungspotenzial von P- und S-Wellenseismik wird demonstriert. Das Zusammenspiel von Seismik und Widerstandsmethoden ermöglicht die Ansprache von grundwasserführenden und grundwasserhemmenden Schichten bis zu einer Tiefe von 150 m.

**Schlüsselwörter** Reflexionsseismik · Widerstandsverfahren · P-Wellen · S-Wellen · Geophysik

## Introduction

In areas with complex geology and limited knowledge of subsurface structures, the search for suitable well locations can be a challenging task. For sustainable management of groundwater resources, aquifers of reasonable size, protected by low permeability layers (e.g., clay or till) that prevent contaminant migration from the surface, are required. In glacially-influenced sedimentary areas, common in the North European Lowlands, the layered structure of aquifers and protective layers are disturbed by, e.g., glaciotectonics or deeply incised glacial valleys (e.g., Aber and Ber 2007; Jørgensen et al. 2009, 2012; Huuse and Lykke-Andersen 2000; Stackebrandt 2009). Interpolation of drilling results can therefore be difficult or impossible even over short distances, increasing the risk of unsuccessful exploratory drilling. For example, in the Hamburg-Baursberg/Sülldorf groundwater development area, experience shows that the probability of locating a suitable well site by exploration drilling is currently only 42% (Skowronek personal communication).

Geophysical methods for near-surface and hydrogeophysical applications have been improved significantly over the last few decades (e.g., Butler 2005; Rubin and Hubbard 2005; Pellerin et al. 2009; Binley et al. 2015). While resistivity methods are widely accepted for delineating aquifers and aquitards or groundwater salinity, seismic methods are only used sporadically in the exploration and development of groundwater resources. This is probably due to the high costs, ambiguity in the results and interpretative difficulties. Large-scale investigations can often only be carried out in connection with research projects (e.g., BURVAL Working Group 2009). Convincing and meaningful studies concerning application of S- and/or P-wave seismic reflections in northern Germany, Denmark and Canada were presented by, e.g., Polom et al. (2013), Krawczyk et al. (2012, 2013), Pugin et al. (2009, 2013); in combination with airborne electromagnetic surveys by Burschil et al. (2012a, b), Jørgensen et al. (2012), Høyer et al. (2013), Tamiru and Wiederhold (2020); and in combination with direct-push by Hoffmann et al. (2008). Recently Sun et al. (2020) demonstrated the imaging of shallow groundwater resources in glacial deposits by high frequency data using an explosive seismic source.

The primary hydrogeologic questions concern the detection of protective covering layers and the minimization of the exploration risk by understanding the subsurface structures and complexity. In this context the objective of our paper is to communicate the combination of seismic and resistivity methods and the advantage of geophysics to address hydrogeologic questions. We demonstrate in this paper the application of geophysical techniques (seismic and resistivity) to define the subsurface architecture in terms of permeable and low-permeable layers for two locations, one in Jutland (Denmark) and one at the northern boundary of Hamburg (Germany) (Fig. 1). P-waves are used at both locations complemented by a shear wave survey at the location Hamburg-Sülldorf. For 2D resistivity imaging we use electrical resistivity tomography and a newly developed mobile transient electromagnetic system (tTEM) (Auken et al. 2019). The added value of our work is the delineation of a buried valley structure in the Hamburg-Sülldorf area and of a thrust structure in the Varde area.

## Study areas

The two selected study areas are located in glacially formed landscapes in western Denmark and in northern Germany (Fig. 1). Both areas have been overridden by glaciers during the Elsterian and Saalian glaciation but the Last Glacial Maximum (Weichselian glaciation) reached only a line eastward of our study areas (Fig. 1a) (Ehlers et al. 2011; Houmark-Nielsen 2011). A good overview on a glaciotectonic thrust-fault complex in the North Sea is given by Winsemann et al. (2020) whereas González et al. (2021) show the internal structure of a push moraine in the Elbe-Weser region close to the Hamburg-Sülldorf location.

The Danish study site, Varde, belongs to the Varde hill-islands where deeply rooted glaciotectonism is recognized. The hill-islands contrast the flat outwash plains as elevated, gently undulating landscapes often consisting of till. The elevated terrains are remnants of an old, pre-Weichselian landscape altered by fluvial, periglacial and postglacial processes (Høyer et al. 2013).

The German study site, Hamburg-Sülldorf, is characterized by an alternating, partly glacially compressed sequence of Quaternary sands, gravels, silts, clays and till. The Qua-

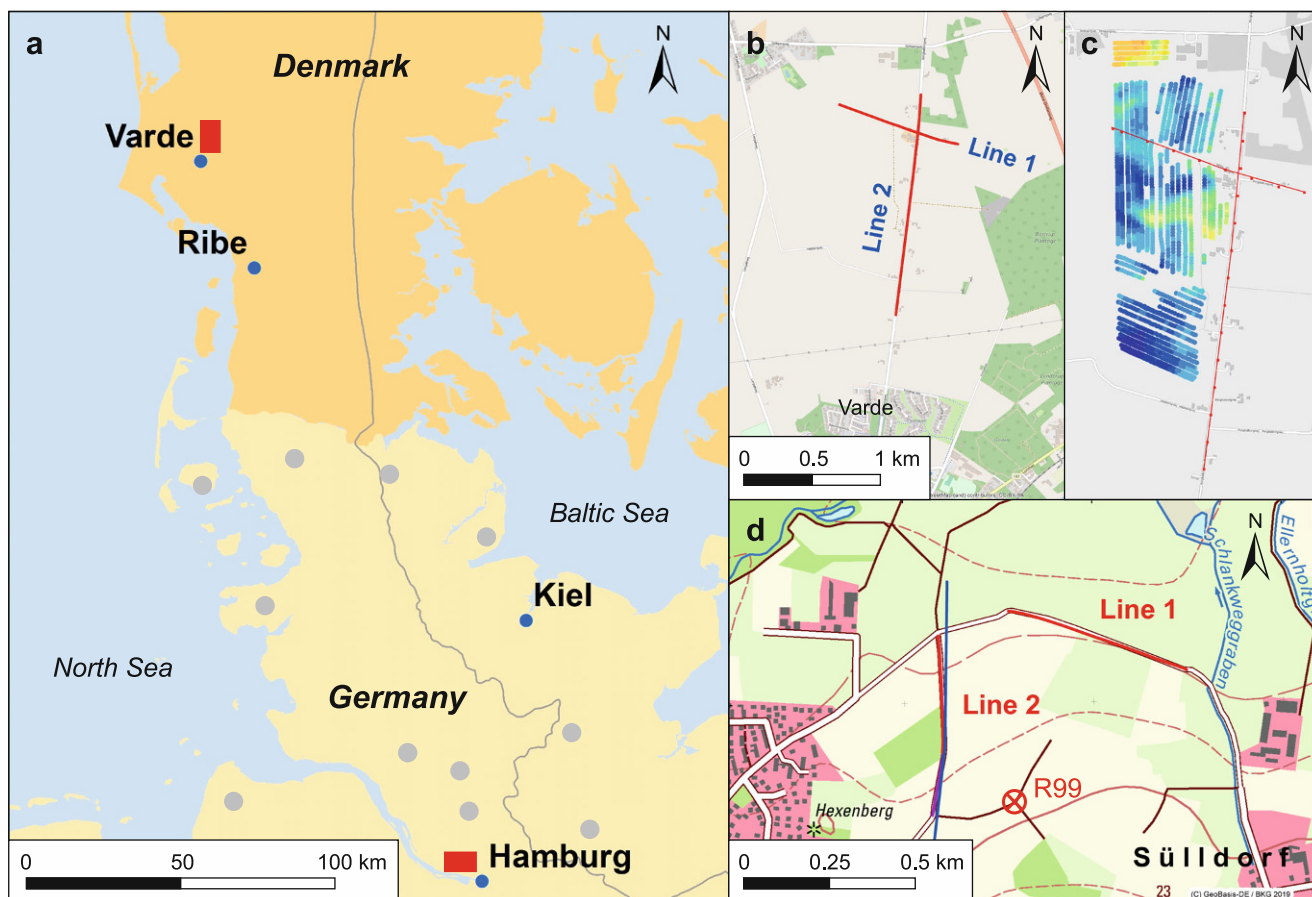


**Fig. 1** **a** Red rectangles show the location of the Varde and Hamburg-Sülldorf study areas (grey line: Last Glacial Maximum; grey dots: locations of high-resolution seismic profiles acquired by LIAG since 1997), **b** Varde—seismic lines, **c** Varde—tTEM lines, resistivity distribution in the interval -15 to -20 m m.s.l. (for color scale see Fig. 3), **d** Hamburg-Sülldorf—seismic lines (red) and ERT line (blue)

**Abb. 1** **a** Rote Rechtecke zeigen die Lage der Untersuchungsgebiete Varde und Hamburg-Sülldorf (graue Linie: Letzteiszeitliches Maximum; graue Punkte: Lage hochauflösender seismischer Profile, die vom LIAG seit 1997 vermessen wurden), **b** Varde – seismische Linien, **c** Varde – tTEM-Messlinien, Widerstandsverteilung in -15 bis -20 m NHN (Farbskala siehe Fig. 3), **d** Hamburg-Sülldorf – seismische Linien (rot) und ERT-Linie (blau)

ternary sequence, which is between 80 and 120 m thick, is underlain by more than 120 m of Miocene mica clay. Up to 150 and 350 m deep Quaternary channels with variable channel filling are known southwest- and southeastward of the area, respectively (Skowronek, personal communication).

## Methods

In our study, we used resistivity methods, as they offer a layer characterization in terms of sandy and clayey material (if there is no saline groundwater), combined with seismic methods, as they provide information about the layer structure of the subsoil.

## Resistivity methods

Resistivity methods are very suitable for porous aquifer investigations because typical groundwater-bearing, coarser-grained layers (e.g., sand, gravel) can be distinguished from protective or interlying, typically fine-grained layers (e.g., clay, till) due to the differences in their resistivity values (Kirsch 2009): Freshwater-filled sandy aquifers have much higher electrical resistivities (80–200  $\Omega$ m) than clay or salt-water saturated layers (2–30  $\Omega$ m).

The method of geoelectrical resistivity imaging is widely known as electrical resistivity tomography (ERT). The field layout consists of a four-electrode arrangement, by which electrical current is injected between two electrodes, and the potential difference is measured between another pair of electrodes. Such measurements are repeated for different combinations of electrodes, thus 2D data coverage along a profile is obtained. ERT may be applied at a wide range

of spatial scales to determine hydrogeological properties but also to determine states, such as volumetric water content or solute concentration (Ferré et al. 2005).

Electromagnetic measurements also provide information on the resistivity structure similar to ERT, but use a different technique (e.g., Christiansen et al. 2009). An electromagnetic field (AC or DC) is produced by an antenna and induces a secondary EM field in the subsurface. Measurements in the frequency domain (e.g., the Slingram approach) use the comparison of the AC primary and secondary electromagnetic field to derive the resistivity distribution of the subsurface, while measurements in the time domain use the rate of change of the secondary field after abruptly turning off the DC current in the transmitter coil (TEM, transient electromagnetics).

A new development in the field of time-domain EM is the tTEM-system, using a towed, ground-based, transient electromagnetic system, designed for detailed 3D geophysical and geological mapping of the shallow subsurface (0–80 m) in a fast and cost-efficient way (Auken et al. 2019; Maurya et al. 2020; Sandersen et al. 2021). An all-terrain vehicle carries the instrumentation and tows the transmitter frame and the receiver coil which are mounted on sleds for a smooth ride over rough terrain. Detailed 3D coverage is obtained by fast data acquisition (working speed is 15–20 km/h) and close line spacing of typically 10–25 m. This results in a dense lateral data spacing with an in-line distance between the soundings of 5–10 m. Such a high resolution cannot be achieved with electromagnetic airborne systems (e.g., SkyTEM), which are often favored for a 3D coverage of large areas (e.g., Siemon et al. 2009).

## Seismic reflection method

Seismic reflection techniques have been well known and accepted for oil and gas exploration for about 100 years. Near-surface applications started with refraction techniques but since 1980 significant progress has been made in seismic reflection surveying (Steeple 2005). In the beginning, P-waves (compressional waves) were mainly created by explosives or weight drops, but nowadays seismic vibrators of different sizes are at hand and can be used for P-wave as well as for S-wave (shear wave) surveys (e.g., Krawczyk et al. 2012, 2013; Polom et al. 2013; Tamiru and Wiederhold 2020). These studies also show that seismic reflection methods work quite well in the unconsolidated sediments of the North European Lowlands despite only minor velocity contrasts between layers.

Seismic methods are sensitive to the velocity and density structure of the subsurface. The field layout is based on the transmission of seismic signals from an energy source and the measurement of the signals at receivers (geophones) at different distances. P- and S-waves differ in the particle mo-

tion of the wave propagation when travelling through earth material. Due to their lower propagation velocity, S-waves have a shorter wavelength than P-waves leading to a better resolution of small subsurface structures given the same frequency content.

The subsoil material of our study areas mainly consists of sand, till and clay. Although these materials seem to be quite similar, in general surprisingly good seismic reflections at layer boundaries occur. The main condition for reflected seismic waves at a layer boundary is that the layers must have different impedance values (the product of density and seismic velocity). Density and seismic velocity depend on porosity, both decrease with increasing porosity. In general, sand, clay and till have different porosities and thus different densities and seismic velocities. The porosity of sand is 20–40% depending on the grain-size distribution. The porosity of clay can be up to 70% due to the high content of immobile water (low effective porosity). The porosity of till (mainly composed of sand and clay) depends on the clay content: if the volumetric clay content is low (up to ca. 30%), then the till porosity is lower than the porosity of sand (Marion et al. 1992), otherwise the porosity will approach the high porosity of clay. Usually, the clay content of till is low, so density and seismic velocity higher than the seismic velocity of sand can be expected, leading to good reflection results.

The field equipment for the P- and S-wave surveys in this study, and examples of seismic wave fields, are shown in Fig. 2. In the Varde survey, the P-wave Vibrator HVP30 (developed by the Leibniz Institute of Applied Geophysics (LIAG)) was used as the seismic source, while the seismic waves were recorded by an array of planted geophones. In the Hamburg-Sülldorf survey P- and S-vibrators ELVIS (originally developed by LIAG) were used with the geophones for P-wave and a SH-landstreamer (SH indicates horizontally polarized shear waves) for the S-wave data recording (Table 1).

Data processing comprises standard first arrival refraction analysis and common-midpoint (CMP) processing. The following steps are included: raw data preparation (vibroseis correlation, quality control, stack shots, assign geometry), prestack processing (true amplitude recovering, automatic gain control AGC, spectral balancing, refraction statics, residual statics, bandpass filter), dynamic correction (normal moveout and dip moveout correction, bottom mute, CMP stacking), and poststack processing (finite difference time migration, deconvolution, time-depth conversion). Standard routines are used as described, e.g., by Yilmaz (2001). The S-wave data processing includes a velocity filter (FK-filter) but no dip moveout correction.

**Fig. 2 a–e** P-wave technique and data: **a** P-wave Vibrator HVP30, **b** planted geophone, **c** single shot gather with AGC (300 ms), spectral balancing and static correction, **d** additionally muting of noise cone applied, **e** power spectrum in decibels; **f–j** S-wave technique and data: **f** SH-Vibrator ELVIS-7, **g** land-streamer, **h** single shot gather with AGC (250 ms) and spectral balancing, **i** additionally FK-filter, deconvolution and bandpass (20–25–90–120 Hz) applied, **j** power spectrum in decibels. SP marks the seismic source position

**Abb. 2 a–e** P-Wellen, Technik und Daten: **a** P-Wellen-Vibrator HVP30, **b** gestecktes Geophon, **c** Einzelschussdarstellung mit AGC (300 ms), Spektralausgleich und statischer Korrektur, **d** zusätzlich Elimination des Noisekegels, **e** Leistungsspektrum in Dezibel; **f–j** S-Wellen, Technik und Daten: **f** SH-Vibrator ELVIS-7, **g** Geophone in Streamer angeordnet, **h** Einzelschussdarstellung mit AGC (250 ms) und Spektralausgleich, **i** zusätzlich FK-Filter, Dekonvolution und Bandpassfilter (20–25–90–120 Hz), **j** Leistungsspektrum in Dezibel. SP markiert die Position der seismischen Quelle

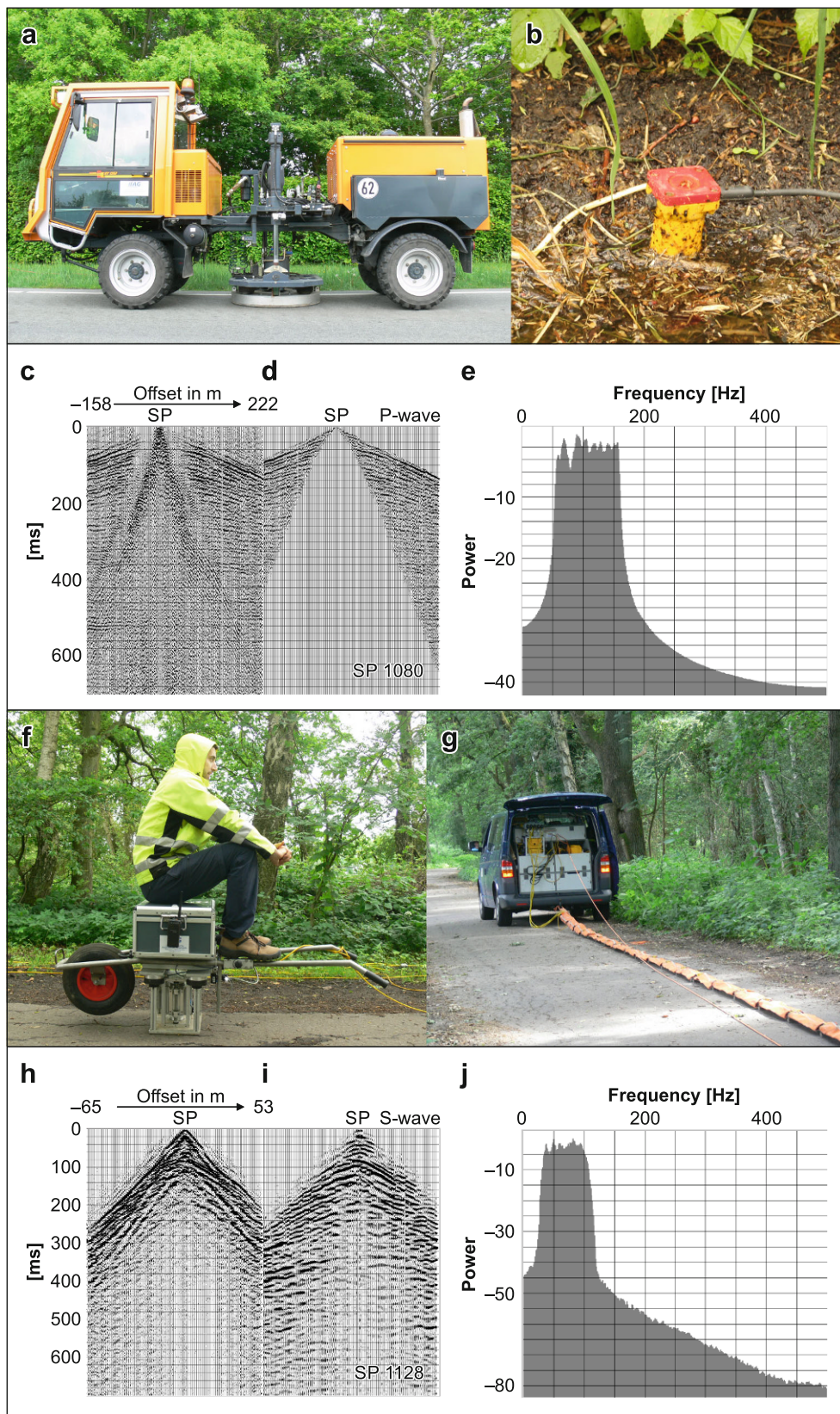


**Table 1** Acquisition parameters of the seismic surveys**Tab. 1** Akquisitionsparameter der Seismikmessungen

Area	Varde <i>P</i>	Hamburg-Sülldorf <i>P</i>	Hamburg-Sülldorf <i>S</i>
Seismic source	LIAG Vibrator HVP30	P-Vibrator (ELVIS-P, electrodynamic vibrator system)	SH-Vibrator (ELVIS-7, electrodynamic vibrator system)
Source signal (sweep)	20–200 Hz, 10 s	20–160 Hz, 10 s	20–160 Hz
Vertical stack	Line 1: 2/Line 2: 3	2	2
Source spacing [m]	5	2	2
Receiver spacing [m]	2.5	2	1
No. of channels	360	278	120
Measurement period	May 24th–27th 2016	June 3rd–6th 2019	July 1st–2nd 2020
Crew members	4	4	4
Profile length (total)	Line 1: 925 m Line 2: 1635 m	Line 1: 547 m Line 2: 341 m	– 528 m
CMP-spacing [m]	1.25	1	0.5

## Approach and results

The exploratory approach that we are pursuing to assess potential groundwater extraction sites is based on overview measurements with P-waves, possibly refinement with S-wave measurements (see case 2) and application of resistivity methods to determine the aquifer properties.

### Case 1: Varde (glacial thrust structure)

The Varde study site is close to the town of Varde, located in the southwestern part of Jutland, Denmark (Fig. 1). The area is prone to a lack of clean groundwater. Nitrate and pesticides often contaminate the shallow aquifers and it has been a challenge in recent years to identify new uncontaminated aquifers. Recent investigations show that the area is glacially heavily deformed with thrusting and folding of subsurface units. This means that pathways for contaminant migration along these structures to the aquifers frequently exist in the area.

In the course of geophysical exploration, a seismic reflection survey was carried out in the Varde area by LIAG in 2016. The acquisition parameters are listed in Table 1. A tTEM survey, carried out by the HydroGeophysics Group of Aarhus University, followed in 2019. Further exploration included a SkyTEM survey and a pumping test. The first with a focus on deeper structures and the latter to check hydraulic properties.

The seismic section shows structural information down to a depth of about 1000 m. At depths below about –100 m (meters below m.s.l.) the seismic reflectors are more or less horizontal and continuous (Fig. 3b). With reference to Høyer et al. (2013), whose survey area is about 20 km further north, we interpret the deep reflectors as the top of the Arnum Formation (Miocene), the top of the Paleogene deposits and the top of the Cretaceous deposits (Fig. 3b). At depths above –100 m, the reflectors show stronger topo-

graphic variation, which presumably indicate a glacioteconic deformation.

The bulged structure in the northern part of seismic line 2 (starting at about profile meter 1000) might be interpreted as a thrust fault. From the appearance of the reflections in both seismic sections, the direction of stress seems to be from the NNE. It is not clear whether the buckling of reflector “A” in continuation to the south results from glacioteconic or erosional forces. Unfortunately, the decollement or thrust plane is not clearly seen (reflector “B” in Fig. 3c).

The seismic velocities increase with depth, but there are only very slight lateral variations in the glacially affected part (Table 2). In the northern part the velocities are slightly higher. The interval velocities calculated from stacking velocities are relatively low in the first layer (above reflector “A”) ranging from 1300 to 1500 m/s. Below reflector “A” the interval velocity values are significantly higher than 1500 m/s (Table 2).

The resistivities gained from the tTEM survey show information down to nearly –120 m (below m.s.l.) (Fig. 3a). The maximum depth of reliable data-supported information is about 60 m. Two ranges of resistivities are clear: the high resistive top layer and the lower resistive bottom layer. The latter rises to the north. The layer boundary (marked with “A”) correlates quite well with the prominent reflector “A” in the seismic section (Fig. 3a, c). The high-resistive top layer is interpreted as a buried valley with a sandy infill. The resistivity depth section reveals that no low-resistive (i.e. protective) covering layer is present.

### Case 2: Hamburg-Sülldorf (glacial valley)

Similar to the Varde area, new well fields are required in the metropolitan area of Hamburg, to ensure a reliable water supply. The targeted aquifer is fine-grained and has low yields. In addition, due to the location in an area of pushed moraines, tilted to steeply standing compressed layers and

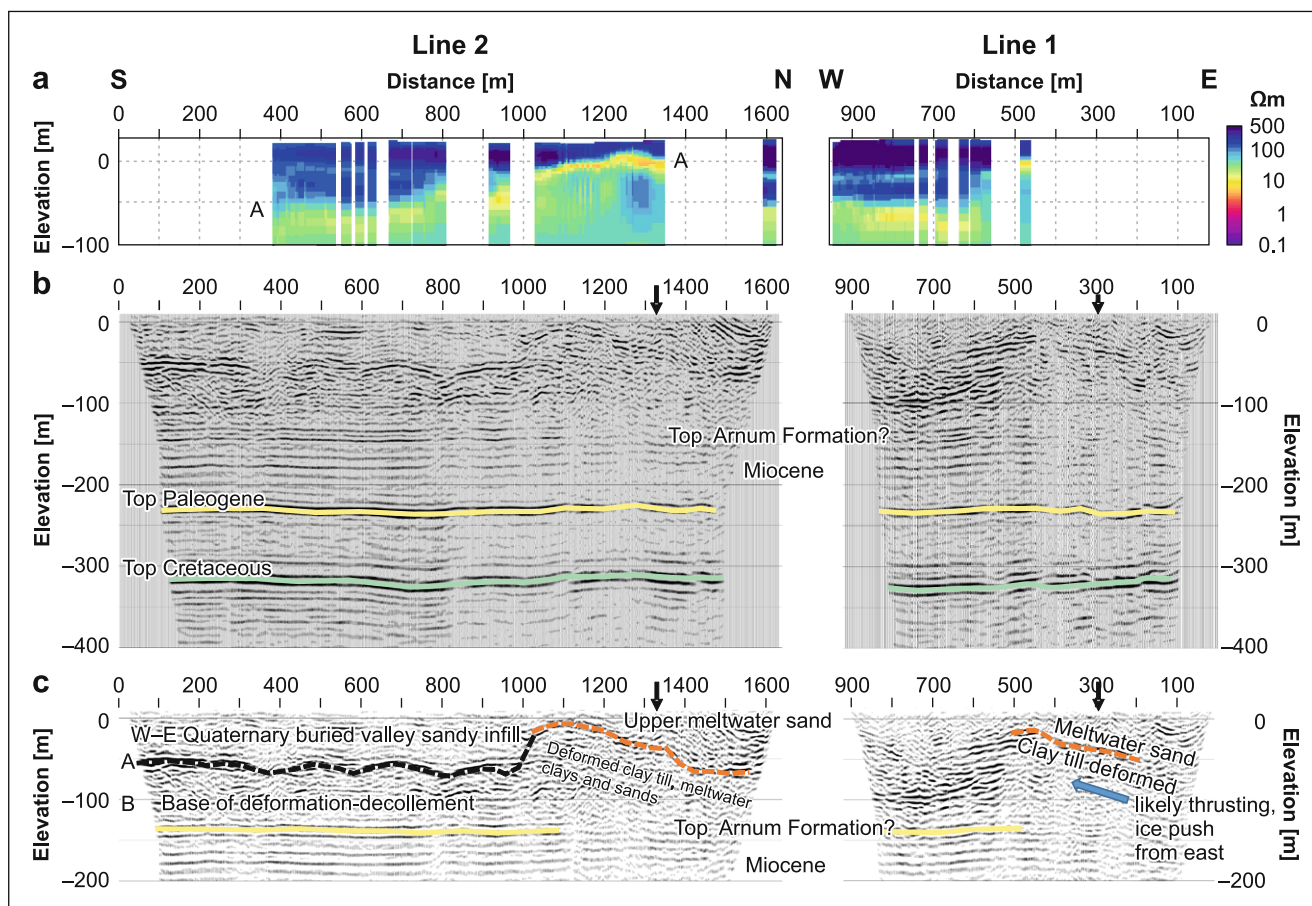


**Fig. 3** Compilation of results for the Varde study area: **a** resistivity depth section from the tTEM survey; **b** P-wave depth section, datum level is 20m above m.s.l., the arrows mark the intersection of the lines; **c** top 200m of **b** with geological interpretation. (H:V = 1:2)

**Abb. 3** Zusammenstellung der Ergebnisse für das Untersuchungsgebiet Varde: **a** Vertikalschnitt des spezifischen elektrischen Widerstands aus der tTEM-Messung; **b** seismische Sektion (P-Welle); Bezugsdatum ist 20m NHN, die Pfeile markieren den Kreuzungspunkt der Profile; **c** obere 200m aus **b** mit geologischer Interpretation. (H:V = 1:2)

possibly embedded mica clay lenses are to be expected. Accordingly, there is a considerable exploration risk and a significant risk of total failure in this area (i.e. of finding no productive groundwater zones). With the use of geophysical techniques, a substantial reduction of the exploration risk is expected.

In June 2019, two seismic profiles with a P-wave seismic source (ELVIS P) were carried out by LIAG in the Hamburg-Sülldorf area. A follow-up survey with S-waves (ELVIS S) was carried out in 2020 with the aim of achieving a higher resolution of the layered structure. For acquisition parameters, see Table 1. Several ERT lines are available from a service company.

The difference between the P- and S-surveys is clearly shown in the recorded seismic wave field (Fig. 2c, d, h, i). In the P-wave survey, the traces of the geophones close to the seismic source are dominated by noise from the source, ground roll (surface wave energy) and the air blast (Fig. 2c). No reflected signals are visible in this zone. This means that the minimum depth of layers which can be imaged

by P-seismic is about 30m. In the S-wave survey, early (=shallow) reflected signals are clearly seen close to the source position (Fig. 2h). The reason is that the noise travelling in the longitudinal direction and the air blast are not recorded by the SH-geophones which are more sensitive to horizontal oscillations. Working on paved ground leads to suppression of the surface waves. Even shallow layers can therefore be detected by S-wave surveys. P- and S-waves also differ in their signal frequency as shown in the power spectra. In our example, for P-waves most seismic energy is in the 50–150 Hz frequency range, for S-waves it is between 30 and 100 Hz.

The P-wave seismic reflection profiles show a two-part picture (Fig. 4c, d). The upper part, down to a depth of about 100m below m.s.l., is characterized by chaotic layering, while the lower part is characterized by a uniform, parallel reflection pattern. This continuous layering is presumably attributable to Neogene or Miocene strata. Further up, horizontal reflections end at the presumed edge of an incised channel (e.g., line 1 at the north side and line 2 at the

**Table 2** Geophysical parameter interval velocity ( $V_P$ ,  $V_S$ ) and resistivity ( $\rho$ ) derived for the study areas  
**Tab. 2** Geophysikalische Parameter Intervallgeschwindigkeit ( $V_P$ ,  $V_S$ ) und Widerstand ( $\rho$ ) abgeleitet für die Projektgebiete

Study area	Base reflector	Lithology	$V_P$ [m/s]	$V_S$ [m/s]	$\rho$ [ $\Omega$ m]
Varde	Above A	Sand (interpreted from tTEM data)	1300–1500	–	> 100
Varde	Below A	Clay (interpreted from tTEM data)	1600–1800	–	20–30
Hamburg-Sülldorf	–	Sand	1700–1900 (no further resolution)	400–500	> 50
Hamburg-Sülldorf	–	Till		> 500	20–30
Hamburg-Sülldorf	–	Miocene clay (mica clay)		–	5–20

east side). The channel-like structures are marked in violet. Line 1 runs more or less perpendicular to the strike of the channel. The channel seems to have different phases, the younger one shows asymmetric filling. Strong horizontal reflections inside the valley (marked in blue) might indicate thick till layers as known, e.g., from borehole R99 (for location see Fig. 1).

The shear wave section shows much less depth penetration but represents the till layer in more detail. The base reflection of the till is especially well displayed (blue line in Fig. 4b at about –50 m relative to m.s.l.), and the S-wave section shows additional information in the upper 20 m. Here a small additional valley structure in the distance range from 120 to 200 m is a good example of the near-surface resolution that is possible with shear waves (black and white color in Fig. 4b).

The seismic velocities derived from stacking velocities are not robust enough for a material interpretation. Here the electrical resistivity is a much more meaningful parameter; the data are displayed in Fig. 4a, d and Table 2. For better correlation, the valley as interpreted in the P-wave section and a prominent deeper reflection, are also shown in the resistivity section. The deep reflection at about –120 m correlates quite well with the low-resistivity layer (<20  $\Omega$ m) that represents clay and thus is interpreted as the top of the Miocene mica clay. Reflections above and outside the valley might be interpreted as Pleistocene and probably Pliocene sands (yellow reflectors). Inside the channel, resistivities higher than 50  $\Omega$ m indicate freshwater-bearing sands, a possible aquifer. Lower resistive regions above, in the depth range down to elevations of –50 m, correlate well with the strong reflections that were interpreted as glacial till. The resistivities support this interpretation. Further above, a thin sand layer is well protected by an overlying clay layer. The very high resistivities on top represent the unsaturated zone and the layer boundary correlates well with the refractor depth indicating groundwater level.

## Discussion

The investigations add valuable knowledge on the subsurface conditions that could not be obtained in this way from

scattered boreholes. The area north of Varde was, based on the geophysical investigations (seismic, tTEM and additional SkyTEM), interpreted to be affected by rather deep glaciotectionics. This is in accordance with results of a test drilling and a pumping test, which revealed an irregular aquifer within thrust layers resulting in surface pollution entering the aquifer. Due to these conclusions, this area was not found feasible for a future water supply. Instead, the target area was shifted towards a buried valley system northwest of Varde, where a more homogeneous sand aquifer within the valley was mapped by the SkyTEM survey and a new well field within this valley is now being developed.

In the Hamburg-Sülldorf area, the valley structure is recognized in line 1 by a sub-horizontal reflection pattern (Fig. 4c, d). Line 2 probably runs at an acute angle to the strike of the valley and the northern flank might be observed in the data. In the S-wave section the till layer and especially its base are well-displayed at about –50 m m.s.l. (Fig. 4b). Deeper reflections are weak. The fact that the strong reflection at about –50 m m.s.l. is weak or interrupted along the distance ranging from 150 to 250 m might be caused by the small depression shown above that scattered the seismic energy and shielded the mapping of deeper horizons. S-waves are more sensitive to scattering due to their shorter wavelength. However, the resistivities also show a gap within the presumed till layer with resistivity values between 20 and 30  $\Omega$ m. In the P-wave section, corresponding reflections are disturbed. Both indicate an interruption of the glacial till with the possibility of reduced aquifer protection.

Seismic velocities are better resolved for S-waves than for P-waves due to the lower velocities and longer travel times of S-waves. Therefore, P-wave velocities show only little variation, while the S-wave velocity analysis indicates higher interval velocities for the glacial till. This is supported by logging results of the exploration borehole ABBAU-2 located about 1000 m southwest of observation well R99 (Fig. 1). An upper till layer and a lower silt/clay (mica clay) layer, both embedded in a sandy environment, are clearly indicated by higher gamma activities due to their clay content. The density log shows increased densities for the till layer. However, no significant density contrast between sand and interlayered silt/clay is observed (Fig. 5a).



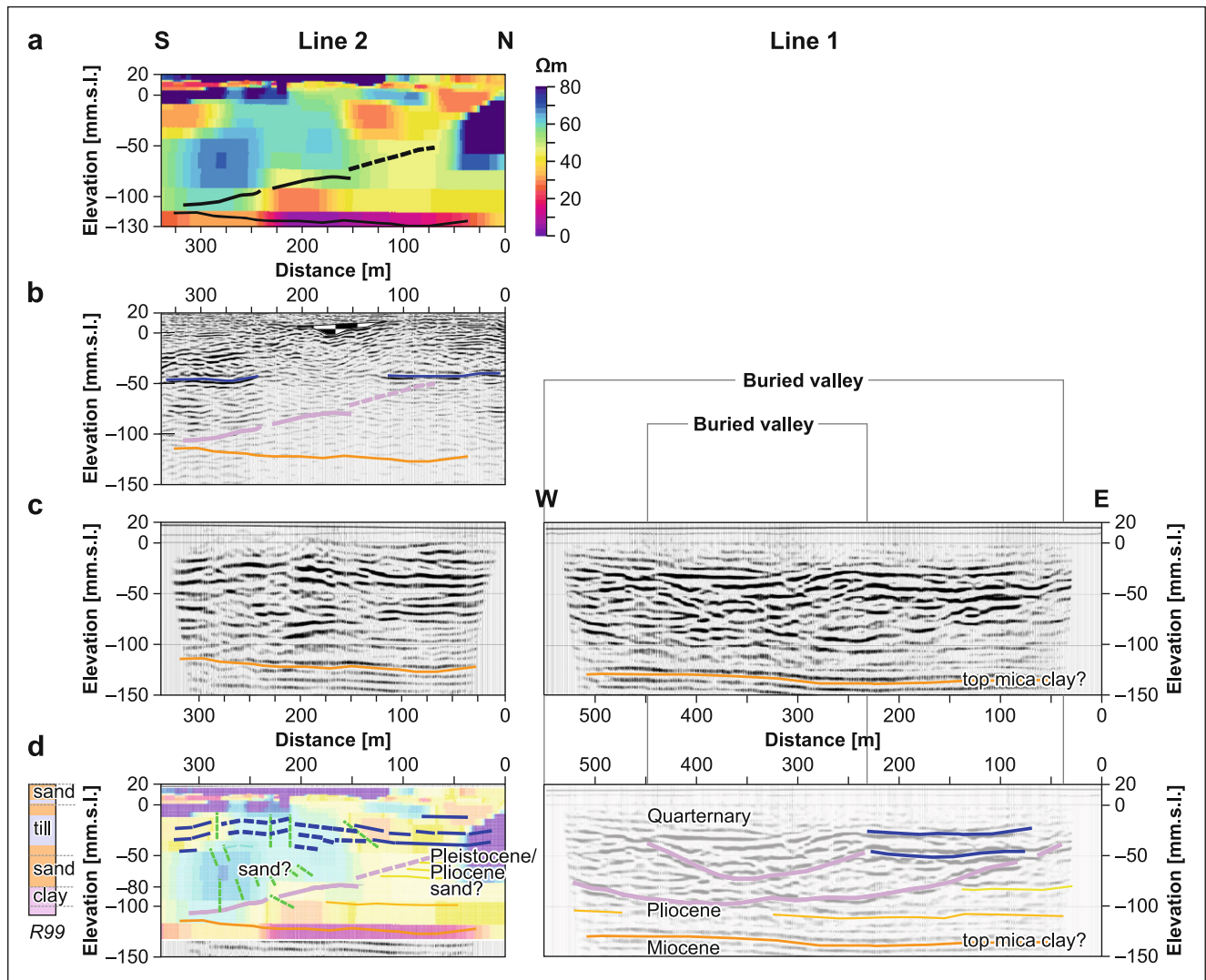


**Fig. 4** Compilation of results for the Hamburg-Sülldorf study area: **a** resistivity depth section from the ERT survey, **b** S-wave depth section, **c** P-wave depth section, datum level is 20m above m.s.l., **d** same as **c** but with interpretation and, for line 2, resistivity from **a**. The violet lines mark the bottom of buried valley structures and the deeper line represents the base of the Quaternary. Borehole R99, which is 250m away, is displayed on the left edge of the picture. The Miocene mica clay is drilled there at -80m m.s.l. (H:V = 1:2)

**Abb. 4** Zusammenstellung der Ergebnisse für das Untersuchungsgebiet Hamburg-Sülldorf: **a** Vertikalschnitt des spezifischen Widerstands aus der ERT-Messung, **b** seismische Sektion (S-Welle), **c** seismische Sektion (P-Welle); Bezugsniveau ist 20m NHN, **d** wie **c** aber mit Interpretation, und im Fall von Profil 2 sind auch die Widerstände aus **a** überlagert. Die violetten Linien markieren die Unterseite von Rinnenstrukturen und die untere bildet die Quartärbasis ab. Am linken Bildrand ist die Bohrung R99 eingeblendet, die sich in 250m Entfernung befindet. Der miozäne Glimmerthon ist dort in -80m NHN erbohrt. (H:V = 1:2)

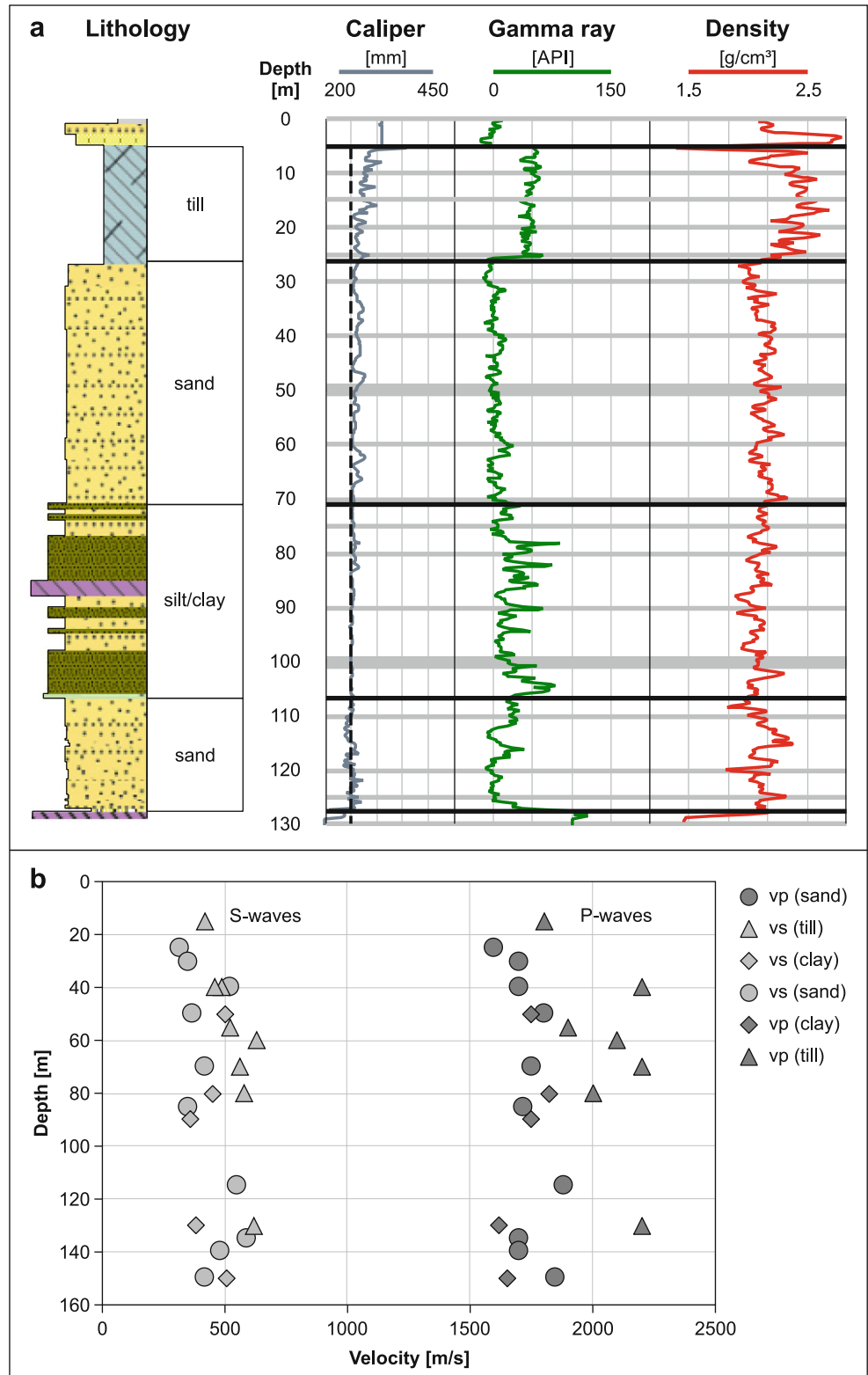
For comparison, we show in Fig. 5b seismic velocities for sand, clay and till layers from VSP (vertical seismic profiling) measurements. The measurements were carried out on the island of Föhr (Burschil et al. 2012b) and in the glacial valley Ellerbeker Rinne (Rumpel et al. 2005) about 25km north of the Hamburg-Sülldorf area. As expected, P-wave velocities for till layers are clearly higher than velocities for sand layers. With one exception (circle and triangle at 40m depth around 500m/s in Fig. 5b) this is also valid for S-wave velocities. As already indicated in the

density log, significant velocity differences between sand and clay are not observed in these VSP data (Fig. 5b).

The resistivity values are much more meaningful with respect to the aquifer properties than the seismic velocities. Due to the surface electrical conductivity of clay minerals, even a minor clay content of the material reduces the electrical resistivity significantly (Table 2).

The various data were processed independently. The relatively good match of the depth of the Miocene mica clay in the P-wave seismic and resistivity data suggests trustworthy processing. Slight discrepancies of resistivity and

**Fig. 5 a** logs from borehole ABBAU-2 in the Hamburg-Sülldorf area: lithology, caliper, gamma ray, density; **b** mean velocity values ( $V_P$  and  $V_S$ ) from VSP data from northern Germany for sand (circles), till (triangles) and clay (rhombs)  
**Abb. 5 a** Logs der Bohrung ABBAU-2 im Messgebiet Hamburg-Sülldorf: Lithologie, Kaliber, Gamma, Dichte; **b** mittlere Geschwindigkeitswerte ( $V_P$  und  $V_S$ ) aus VSP-Daten aus Norddeutschland für Sand (Kreise), Geschiebemergel (Dreiecke) und Ton (Rauten)



seismic data (especially in the Varde case) can be attributed to deviations in the survey lines.

## Conclusion

We showed the application of geophysical methods to locate potential groundwater extraction sites for two areas and presented a qualitative interpretation. The geological structure was revealed in both areas by the geophysical investigations. In the Varde area a sandy channel filling could be separated from a glaciotectionic thrust structure. Test drilling and a pumping test revealed an irregular aquifer with only a limited protective cover which would result in a considerable vulnerability of the aquifer due to contamination from the surface. In Hamburg-Sülldorf a buried valley structure was identified, the existence of which was not formerly known. Neogene and Quaternary facies were distinguished, and sedimentary or erosional features are now better understood, a prerequisite for a successful drilling campaign. The differentiation of the top of the Miocene clay, Neogene sands, and a Quaternary channel with internal structure was possible with the presented geophysical investigations.

In both areas the combination of seismic depth sections with resistivity data has greatly increased knowledge on the subsurface architecture. At the Varde site, for example, only the geophysical surveys could provide the information that was required for rejecting the site for water supply. For the Hamburg site, only the geophysical survey could provide the required information which was necessary to understand the subsurface architecture. Here, too, the findings are guiding the development of the new well field and the site of the next exploration drilling. The approach using a P-wave survey for the first overview, a refinement by a S-wave survey and additionally the use of resistivity methods for addressing the material properties was successful and is recommended for future seismic surveys in comparable areas.

**Acknowledgements** The TOPSOIL project is co-funded by the Interreg North Sea Region Programme (J No 38 2 27 15). The manuscript was significantly improved by the comments and questions from an unknown reviewer and C. Juhlin.

**Funding** Open Access funding enabled and organized by Projekt DEAL.

**Open Access** This article is licensed under a Creative Commons Attribution 4.0 International License, which permits use, sharing, adaptation, distribution and reproduction in any medium or format, as long as you give appropriate credit to the original author(s) and the source, provide a link to the Creative Commons licence, and indicate if changes were made. The images or other third party material in this article are included in the article's Creative Commons licence, unless indicated otherwise in a credit line to the material. If material is not included in the article's Creative Commons licence and your intended use is not permitted by statutory regulation or exceeds the permitted use, you will

need to obtain permission directly from the copyright holder. To view a copy of this licence, visit <http://creativecommons.org/licenses/by/4.0/>.

## References

- Aber, J.S., Ber, A.: Glaciotectionism. *Developments in quaternary sciences* 6. Elsevier, , p 246 (2007)
- Auken, E., Foged, N., Larsen, J.J., Lassen, K.V.T., Maurya, P.K., Dath, S.M., Eiskjær, T.T.: tTEM—A towed transient electromagnetic system for detailed 3D imaging of the top 70 m of the subsurface. *Geophysics* **84**, E13–E22 (2019). <https://doi.org/10.1190/GEO2018-0355.1>
- Binley, A., Hubbard, S.S., Huisman, J.A., Revil, A., Robinson, D.A., Singha, K., Slater, L.D.: The emergence of hydrogeophysics for improved understanding of subsurface processes over multiple scales. *Water Resour. Res.* **51**, 3837–3866 (2015). <https://doi.org/10.1002/2015WR017016>
- Burschil, T., Wiederhold, H., Auken, E.: Seismic results as a-priori knowledge for airborne TEM data inversion—a case study. *J. Appl. Geophys.* **80**, 121–128 (2012a). <https://doi.org/10.1016/j.jappgeo.2012.02.003>
- Burschil, T., Scheer, W., Kirsch, R., Wiederhold, H.: Compiling geophysical and geological information into a 3-D model of the glacially-affected island of Föhr. *Hydrol. Earth Syst. Sci.* **16**, 3485–3498 (2012b)
- BURVAL Working Group: Buried Quaternary valleys—a geophysical approach. *Z. Dtsch. Ges. Geowiss.* **160**, 237–247 (2009)
- Butler, D.K. (ed.): *Near surface geophysics*. Society of Exploration Geophysicists, Tulsa, p 758 (2005)
- Christiansen, A.V., Auken, E., Sørensen, K.: The transient electromagnetic method. In: Kirsch, R. (ed.) *Groundwater geophysics—A tool for hydrogeology*, 2nd edn., pp. 179–225. Springer, Heidelberg (2009)
- Ehlers, J., Grube, A., Stephan, H.-J., Wansa, S.: Pleistocene glaciations of north Germany—new results. In: Ehlers, J., Gibbard, P.L., Hughes, P.D. (eds.) *Quaternary glaciations—extent and chronology: a closer look*, pp. 149–162. Elsevier, Amsterdam, Boston (2011)
- Ferré, T.P.A., Binley, A., Geller, J., Hill, E., Illangasekare, T.: Hydrogeophysical methods at the laboratory scale. In: Rubin, Y., Hubbard, S.S. (eds.) *Hydrogeophysics*, pp. 441–463. Springer, Berlin Heidelberg (2005)
- González, E., Deus, N., Siemon, B., Elbracht, J.: Structural modelling of the northern Elbe-Weser region and the Lamstedt Push Moraine (Lower Saxony, Germany) supported by helicopter borne electromagnetics (HEM). *Quaternary Sci. J.* (submitted 2021)
- Hoffmann, S., Beilecke, T., Werban, U., Leven, C., Engeser, B., Polom, U.: Integrierter Einsatz von Scherwellenseismik und Direct-Push-Verfahren zur Erkundung eines urbanen Grundwasserleiters. *Grundwasser* **13**(2), 78–90 (2008)
- Houmark-Nielsen, M.: Pleistocene glaciations in Denmark: a closer look at chronology, ice dynamics and landforms. In: Ehlers, J., Gibbard, P.L., Hughes, P.D. (eds.) *Quaternary Glaciations—extent and chronology: a closer look*, pp. 47–57. Elsevier, Amsterdam, Boston (2011)
- Høyer, A.-S., Jørgensen, F., Piotrowski, J.-A., Jakobsen, P.R.: Deeply rooted glaciotectionism in western Denmark: geological composition, structural characteristics and the origin of Varde hill-island. *J. Quat. Sci.* **28**(7), 683–696 (2013)
- Huuse, M., Lykke-Andersen, H.: Overdeepened Quaternary valleys in the eastern Danish North Sea: morphology and origin. *Quat Sci Rev* **19**, 1233–1253 (2000)
- Jørgensen, F., Sandersen, P.B.E.: Buried valley mapping in Denmark: evaluating mapping method constraints and importance of data density. *Z. Dtsch. Ges. Geowiss.* **160**, 211–223 (2009)

- Jørgensen, F., Scheer, W., Thomsen, S., Sonnenborg, T.O., Hinsby, K., Wiederhold, H., Schamper, C., Burschil, T., Roth, B., Kirsch, R., Auken, E.: Transboundary geophysical mapping of geological elements and salinity distribution critical for the assessment of future sea water intrusion in response to sea level rise. *Hydrol. Earth Syst. Sci.* **16**, 1845–1862 (2012). <https://doi.org/10.5194/hess-16-1845-2012>
- Kirsch, R.: Petrophysical properties of permeable and low-permeable rock. In: Kirsch, R. (ed.) *Groundwater geophysics—a tool for hydrogeology*, 2nd edn., pp. 1–22. Springer, Heidelberg (2009)
- Krawczyk, C.M., Polom, U., Trabs, S., Dahm, D.: Sinkholes in the city of Hamburg—New urban shear-wave reflection seismic system enables high-resolution imaging of subsrosion structures. *J Appl Geophys* **78**, 133–143 (2012). <https://doi.org/10.1016/j.jappgeo.2011.02.003>
- Krawczyk, C.M., Polom, U., Beilecke, T.: Shear-wave reflection seismics as valuable tool for near-surface urban applications. *Lead. Edge* **32**, 256–263 (2013). <https://doi.org/10.1190/tle32030256.1>
- Marion, D., Nur, A., Yin, H., Han, D.: Compressional velocity and porosity in sand-clay mixtures. *Geophysics* **57**, 554–563 (1992)
- Maurya, P.K., Christiansen, A.V., Pedersen, J., Auken, E.: High resolution 3D subsurface mapping using a towed transient electromagnetic system—tTEM: case studies. *Near Surf. Geophys.* **18**(3), 249–259 (2020). <https://doi.org/10.1002/nsg.12094>
- Pellerin, L., Holliger, K., Slater, L., Yaramanci, U. (eds.): *Hydrogeophysics—methods and processes*. EAGE Publications, Houten, p 661 (2009)
- Polom, U., Bagge, M., Wadas, S., Winsemann, J., Brandes, C., Binot, F., Krawczyk, C.M.: Surveying near-surface depotcentres by means of shear wave seismic. *First Break*. **31**, 67–79 (2013)
- Pugin, A.J.-M., Pullan, S.E., Hunter, J.A., Oldenborger, G.A.: Hydrogeological prospecting using P- and S-wave landstreamer seismic reflection methods. *Near Surf. Geophys.* **7**, 315–327 (2009)
- Pugin, A.J.-M., Brewer, K., Cartwright, T., Pullan, S.E., Perret, D., Crow, H., Hunter, J.A.: Near surface S-wave seismic reflection profiling—new approaches and insights. *First Break*. **31**, 49–60 (2013). <https://doi.org/10.3997/1365-2397.2013005>
- Rubin, Y., Hubbard, S.S. (eds.): *Hydrogeophysics*. Springer, Dordrecht, p 523 (2005)
- Rumpel, H.-M., Hölscher, F., Grelle, T., Stoll, M.: VSP-Messungen in der Ellerbeker Rinne – Bericht zu Technischer Durchführung und Processing. GGA-Bericht (unpublished), Archiv-Nr. 125 857; Hannover (2005)
- Sandersen, P.B.E., Kallesøe, A.J., Møller, I., Høyer, A.-S., Jørgensen, F., Pedersen, J.B., Christiansen, A.V.: Utilizing the towed Transient ElectroMagnetic method (tTEM) for achieving unprecedented near-surface detail in geological mapping. *Eng. Geol.* (2021). <https://doi.org/10.1016/j.enggeo.2021.106125>
- Siemon, B., Christiansen, A.V., Auken, E.: A review of helicopter-borne electromagnetic methods for groundwater exploration. *Near Surf. Geophys.* **7**, 629–646 (2009)
- Stackebrandt, W.: Subglacial channels of Northern Germany—a brief review. *Z. Dtsch. Ges. Geowiss.* **160**, 203–210 (2009)
- Steeple, D.W.: Shallow seismic methods. In: Rubin, Y., Hubbard, S.S. (eds.) *Hydrogeophysics*, pp. 215–251. Springer, Berlin Heidelberg (2005)
- Sun, R., Kaslilar, A., Juhlin, C.: Reprocessing of high-resolution seismic data for imaging of shallow groundwater resources in glacial deposits, SE Sweden. *Near Surf. Geophys.* **18**, 545–559 (2020)
- Tamiru, G., Wiederhold, H.: P- and S-wave reflection profiling for near-surface investigation of glacial sediments. *J Appl Geophys* **183**, 104216 (2020). <https://doi.org/10.1016/j.jappgeo.2020.104216>
- Winsemann, J., Koopmann, H., Tanner, D.C., Lutz, R., Lang, J., Brandes, C., Gaedicke, C.: Seismic interpretation and structural restoration of the Heligoland glaciotectionic thrust-fault complex: Implications for multiple deformation during (pre-)Elsterian to Warthian ice advances into the southern North Sea Basin. *Quat Sci Rev* **227**, 106068 (2020)
- Yilmaz, Ö.: *Seismic data analysis: processing, inversion and interpretation of seismic data*. Investigations in geophysics, vol. 10. Society of Exploration Geophysicists, Tulsa (2001)

**Publisher's Note** Springer Nature remains neutral with regard to jurisdictional claims in published maps and institutional affiliations.